


A mid-infrared laser absorption sensor for calibration-free measurement of nitric oxide in laminar premixed methane/ammonia cofired flames

Qing Li¹ | Feiyu Ji¹ | Wei Wang¹ | Lihao Ma^{1,2} | Yu Wang^{1,3} 

¹Combustion and Laser Sensing Laboratory, School of Automotive Engineering, Wuhan University of Technology, Wuhan, China

²State Key Laboratory of Applied Optics, Changchun Institute of Optics, Fine Mechanics and Physics, Chinese Academy of Sciences, Changchun, China

³Foshan Xianhu Laboratory of the Advanced Energy Science and Technology Guangdong Laboratory, Xianhu Hydrogen Valley, Foshan, China

Correspondence

Lihao Ma, Combustion and Laser Sensing Laboratory, School of Automotive Engineering, Wuhan University of Technology, Wuhan 430070, China.
Email: liuhaoma@whut.edu.cn

Funding information

Foshan Xianhu Laboratory of the Advanced Energy Science and Technology Guangdong Laboratory, Grant/Award Number: XHD2022-001; National Natural Science Foundation of China, Grant/Award Numbers: 52106221, 51976142; State Key Laboratory of Applied Optics, Grant/Award Number: SKLA02022001A05

Abstract

An interband cascade laser (ICL)-based absorption sensor was developed for calibration-free and high-fidelity measurement of nitric oxide (NO) in laminar premixed methane/ammonia cofired flames using a combination of a micro-probe and a low-pressure, high-temperature gas cell. The developed sensor, which has been shown to be particularly suitable for kinetic studies of ammonia combustion, used a tunable, continuous, narrow-linewidth, free-space ICL operating at $\sim 5.2 \mu\text{m}$ to target the optimal NO transition centered at 1900.07 cm^{-1} . A direct absorption spectroscopy technique with a reduced line model was implemented for calibration-free measurements. Comprehensive experiments were first conducted to evaluate the sensor performance against the standard gas mixture at varied pressure from 20 to 101 kPa at 393 K, showing a relative difference of $\leq 2.5\%$ and a measurement uncertainty of $\leq 2.0\%$. Such a sensor shows a minimum detection limit of $\sim 2 \text{ ppm}$ at the integration time of 1 s. The sensor was then applied for investigating the NO formation in ammonia-methane cofiring flames with various ammonia blending ratios; the acquired experimental data was further used as benchmark data for evaluation of literature chemical mechanisms for ammonia combustion. The developed sensor system was demonstrated to be capable of providing quantitative and spatially resolved measurement of NO in ammonia-methane cofired flames.

KEYWORDS

ammonia/methane cofired flame, calibration-free measurement, high accuracy, minimally intrusive measurement, NO sensor

1 | INTRODUCTION

Ammonia, an efficient hydrogen carrier, is widely recognized as a promising carbon-free fuel that could play an essential role in the near future to decarbonize the energy-intensive industrial sectors that are presently relying on fossil fuels (e.g., power generation, cement, ceramics, glass manufacturing, metallurgy, etc.).¹ By

blending traditional fossil fuels with a high proportion of carbon-free ammonia fuel, CO₂ emissions can be substantially reduced.² Notably, in recent years, successful pilot-scale applications of methane-ammonia cofiring combustion in power boilers and internal combustion engines, as well as pure ammonia combustion in high-temperature industrial kilns have been reported.³ Nevertheless, the high NO_x emissions associated with

ammonia combustion present significant concerns. In this regard, precise measurement of NO_x concentration from ammonia-rich flames plays a vital role both for the understanding the fundamental kinetics of NO_x formation and for monitoring and controlling NO_x emission during the practical ammonia combustion processes.⁴

Over the past decades, various quantitative diagnostic techniques for NO detection have been developed, such as electrochemical method,⁵ nondispersive infrared (NDIR) spectroscopy,⁶ nondispersive ultraviolet (NDUV) technique,⁷ Fourier transform infrared spectroscopy (FTIR),⁸ chemiluminescence detectors (CLD),⁹ and laser-induced fluorescence (LIF).¹⁰ However, applying these methods for NO measurements in methane-ammonia cofiring combustion is challenging. First, unlike conventional hydrocarbon fuels, the complete combustion products of NH₃ are only water vapor (H₂O) and N₂ gas so that its high-temperature combustion products would consist of notably higher concentration of H₂O vapor than that of conventional hydrocarbons.¹¹ It is important to point out here that for methods requiring water condensation and removal, the loss of water vapor can lead to significant distortion in the measurement of NO concentration. For instance, in a nitrogen atmosphere containing 100 ppm of NO and 30% water vapor, the measured NO concentration value can increase to 143 ppm after removing water condensation, resulting in a deviation of 43%. Although possible corrections can be carried out to improve the measurement reliability if accurate knowledge of H₂O is known, additional measurements of H₂O introduce the measurement complexity and uncertainty. More importantly, for ammonia combustion it is also essential to monitor the concentration of residual ammonia in the combustion products due to emission regulations (ammonia is a toxic gas) and the need to evaluate combustion efficiency. However, ammonia is highly soluble in water so that water removal and dry-based measurement is not an option. As such, an electrochemical sensor which requires frequent water removal is not suitable for our measurement target. NDIR and FTIR can provide NO measurement in the presence of high-humidity condition; however, the measurement accuracy suffers significantly from water vapor interferences and correction must be made due to the strong infrared activity of H₂O.¹² NDUV overcomes the water interference issue by transferring the measurements from the infrared region to ultraviolet spectra where H₂O interferences are absent.¹³ However, the accuracy of this method can be strongly influenced by the variation of light intensity.

LIF is a widely used method for in situ measurement of NO. However, it requires a complex mathematical model for quantitative determination of gas concentration,

resulting in measurement with potentially large deviations (due to, for instance, fluorescence quenching).¹⁴ Notably, during ammonia combustion fuel-type NO formation can be pronounced in large amounts (order of magnitude higher than in hydrocarbon combustion) so that LIF signals can be easily saturated, limiting the measurement dynamic ranges. In addition, LIF systems are typically bulky and costly and thus may not be suitable for field tests. CLD is another representative method for NO detection, and it utilizes the chemiluminescent generated from the reaction between NO and ozone (O₃).⁹ However, there are several issues associated with NO_x analyzers that employ CLD, such as the dependence on temperature, and susceptibility to interference in the conversion of NO₂ to NO. In addition, CLD has a limited dynamic range for NO due to sensor saturation. The upper limit for a typical CLD instrument is several thousand ppm, which can't satisfy the requirements of NO detection from ammonia combustion. In addition, it is noted that most aforementioned sensor techniques require frequent calibration which can be cumbersome when continuous measurement is required.

The laser spectroscopic method has garnered extensive utilization in the field of gas sensing.¹⁵ Specifically, laser absorption spectroscopy (LAS) which utilizes the frequency-resolved fractional transmission of incident laser intensity to determine the gas properties has emerged as the preeminent choice.^{16–22} It is based on the interaction between the laser light and the target gas molecules and is a representative technique for gas sensing. By fitting the measured spectrally resolved absorption features, calibration-free and quantitative measurements can be achieved.²³ Over the past decades, LAS has been successfully used for species sensing in laboratory-scale and practical combustion systems.^{24–26} Regarding the NO detection, various studies have been conducted for exhaust from thermal power boilers, engines and shock tubes. However, previous works were mostly related to detection of low concentration NO from hydrocarbon flames. Long-distance multipass gas cells (MPGC) were typically used which was not applicable for ammonia-fueled scenarios due to large amount of NO formation. It is important to mention that extended sampling time while using the MPGC will contribute to distorted results as NO can react with O₂. In addition, accurate measurement of NO using LAS is also challenging because the candidate NO absorption features were contributed by many multifold transitions,^{27–29} introducing the difficulty in accurate fitting of the absorption feature with high efficiency.³⁰

In this work, a mid-infrared laser-based sensor was developed for calibration-free and minimally intrusive

measurement of NO in methane-ammonia cofired flames. An interband cascade laser was adopted to cover the spectra of NO centered at 1900.07 cm^{-1} . A custom-built high-temperature gas cell with a 35 cm path length is designed for ex situ measurements of micro-probe sampled gas mixtures from flames. The gas concentration was obtained from an improved calibration-free direct absorption spectroscopy (DAS) with a reduced line model. The sensor performance was first evaluated against standard gas mixtures and then applied for measuring NO concentration in flames. Kinetic modeling with different chemical mechanisms were also performed and quantitative comparison with the in situ measurement results from literature was presented.

2 | SPECTROSCOPIC FUNDAMENTALS

The NO sensor developed here was based on the theory of LAS and employs a combination of DAS and a reduced line model (to be discussed in Section 3.2) for calibration-free and quantitative determination of gas concentration. The relevant concepts, notation, and abbreviation are briefly presented here in the context of the experiments.

When a collimated and monochromatic laser beam at a certain optical frequency ν (cm^{-1}) travels through a uniform absorbing gas medium with an effective optical absorption length L (cm^{-1}), the fractional attenuation of the laser intensity is governed by the Beer-Lambert relation³¹:

$$\left(\frac{I_t}{I_0}\right) = \exp(-\alpha_\nu) = \exp(-S_i(T)PX_{\text{NO}}\phi_\nu L), \quad (1)$$

where I_0 and I_t are the incident and transmitted laser intensities, respectively; α_ν denotes the spectral absorbance at optical frequency ν [cm^{-1}]; $S_i(T)$ [$\text{cm}^{-2}\cdot\text{atm}^{-1}$] is the temperature-dependent line-strength of the specific ro-vibrational transition i at the gas temperature T ; P [atm] and X_{abs} are respectively the total gas pressure and gas concentration of the absorbing species; and ϕ_ν [cm] is the line-shape function. As ϕ_ν is normalized to unity through integration over the entire transition line, the integrated absorbance (A_i) across the entire absorption feature is expressed as:

$$\begin{aligned} A_i &= \int_{-\infty}^{+\infty} \alpha_\nu d\nu = \int_{-\infty}^{+\infty} (S_i(T)PX_{\text{abs}}\phi_\nu L) d\nu \\ &= S_i(T)PX_{\text{NO}}L. \end{aligned} \quad (2)$$

By scanning the wavelength across the absorption feature, the integrated absorbance can be determined by

Voigt-fitting to the measured spectrum. In this way, the unknown and complicated spectral broadening issue can be eliminated when performing the scanned-wavelength measurements. In this work, the analytical approximation developed by Mclean et al.³² was adopted to achieve efficient and accurate modeling of the Voigt lineshape. The gas concentration can be determined from A_i with the known temperature, pressure, and absorption path length based on Equation (2).

3 | EXPERIMENTAL

3.1 | Line selection

The selection of absorption lines is a critical factor in achieving reliable measurements. Figure 1 depicts the spectral simulation of selected absorption lines based on the HITRAN database³³ for a typical combustion gas. For CH_4/NH_3 cofired flames, H_2O concentration can reach up to 25%–30% which is significantly higher than conventional hydrocarbon fuels. To minimize undesirable spectral interference from water vapor and to avoid a significant reduction in line strength under high-temperature conditions, a specific absorption line must be chosen. As shown in Figure 1A, the absorption line of NO near $5.2\ \mu\text{m}$ can be used as a candidate line due to the good spectral isolation to other species and sufficient line-strength. By involving in the high-humidity environment as illustrated in Figure 1B, it can be seen that the absorption characteristic of NO near 1900.07 cm^{-1} has a considerable intensity and is almost unaffected by major combustion products such as H_2O , CO, and NH_3 . After further validation through spectral

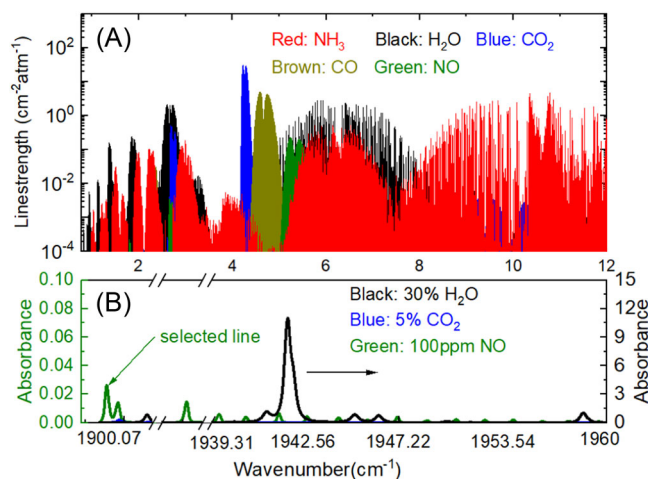


FIGURE 1 (A) Spectral simulation of the selected nitric oxide (NO) absorption lines based on the HITRAN 2010 database.³³ (B) Typical spectral simulation of NO, H_2O and CO_2 for $P = 1$ atm, $T = 393$ K, $X_{\text{H}_2\text{O}} = 30\%$, $X_{\text{CO}_2} = 5\%$, $X_{\text{NO}} = 100$ ppm, $L = 35$ cm.

calculations, we finally selected 1900.07 cm^{-1} for the spectral analysis of direct NO absorption under high temperature.

3.2 | Reduced model

In calibration-free DAS, the gas concentration is determined by fitting the measured absorption features with the best Voigt-fit. During the iterative process of spectral fitting, three spectroscopic parameters including line-center (ν_0), integrated absorbance (A), and collisional broadening width ($\Delta\nu_c$) for each absorption transition, are considered as free parameters in the fitting routine. As a result, the number of free variables is at least three times the number of transitions, leading to an increased chance of pseudo convergence and therefore reduced accuracy and longer convergent time. This issue is particularly evident for absorption features that consist of multifold transitions,³⁰ such as the NO lines selected in this study.

To address this issue, we propose a reduced line model for the calibration-free DAS technique. This approach provides a convenient way to achieve a more efficient spectral-fitting process by reducing the number of absorption transitions involved in spectral calculations while maintaining an acceptable level of accuracy. Specifically, adjacent lines can be replaced by fewer equivalent ones to describe the same absorption spectra without introducing significant errors. Note that the two absorption features near 1900.07 and 1900.51 cm^{-1} can be accessed simultaneously by scanning the laser injection current. To achieve accurate and reliable determination of the integrated absorbance near 1900.07 cm^{-1} , simultaneous Voigt-fitting to the two absorption features is required. Therefore, a reduced line model was built for the two absorption features. For the selected NO spectra near 1900.07 cm^{-1} and the nearby spectra near 1900.51 cm^{-1} , we list the 12 adjacent transitions for the two absorption features in Table 1, taking the line-strength and the lower-state energy (E'') from the most-updated HITRAN 2020 database. The next step is to determine the spectroscopic parameters, namely line-center, line-strength, and lower state energy for the reduced line model. Figure 2A illustrates the calculated spectra of 1000 ppm NO at a pressure of 1 atm and a temperature of 393 K. All 24 lines contribute to two distinguishable absorption features, centered at 1900.07 and 1900.51 cm^{-1} , respectively. It is possible to describe the entire spectra using only two equivalent lines. With the two-line positions determined at 1 atm, the line-strengths of these two equivalent lines are obtained from the best-fit results of the original NO spectra at 1 atm. The lower-state energy is obtained by fitting the equivalent line-strengths at various temperatures. The two new lines proposed in the reduced line model are plotted as dotted drop lines in Figure 2A for comparison. More details

of the spectroscopic parameters are provided in Table 1. At the pressure of 1 atm, Figure 2B compares the calculated absorption spectra of 1000 ppm NO (300, 393 K) using the original 24 lines with the reduced two-line model. The maximum difference is observed to be below 0.3%. The good agreements between the simulation using original 24 lines and the simulations with reduced two-line model reveals that the reduced two lines can reproduce the absorption spectra of NO with acceptable accuracy. In Section 4, we will demonstrate the superior performance of using the two equivalent absorption lines for fast, accurate and robust fitting to the measurement absorption profile.

3.3 | Sensor configuration

Figure 3A depicts the schematic of the optical configuration for the present mid-infrared laser-absorption sensor for NO measurement. A tunable, continuous, narrow-linewidth, free-space distributed feedback interband cascade laser (DFB-ICL, Nanoplus) with an output power of approximately 3 mW at 1900.07 cm^{-1} was employed as the single-mode light source. The operation temperature and injection current were precisely controlled by a commercial low-noise driver (Stanford, LDC 500). By fixing the operating temperature at 24.5°C , the selected absorption feature of NO was swept across by scanning the injection current from 0 to 80 mA at 100 Hz, produced by a software-based function generator. The output laser beam was collimated using by a nonspherical lens (Thorlabs, C036TME-E) and then directed through a custom-built high-temperature gas cell by a flat mirror (PM, $D = 25.4\text{ mm}$). The gas cell was sealed by a pair of calcium fluoride windows with $1\text{--}3^\circ$ wedge. The transmitted laser beam was then collected by concave mirror (Thorlabs, CM254-100-M01, $D = 25.4\text{ mm}$) and focused onto the active area of a mercury cadmium telluride (MCT) photodetector (VIGO system, PVI-3TE-6). A narrow band-pass filter (Favision, BP5230-50 nm) was placed before the photodetector to reduce the emissions from high-temperature flue gases that will contribute to offset signals by filtering the broadband emissions. A multichannel data acquisition module (National Instrument, USB 6363) was used to perform the signal trigger synchronization and data acquisition (200 kHz sampling rate).

All the measurements were performed for flames stabilized on a standard water-cooled McKenna burner with an inner sintered copper (60 mm diameter) shielded by an annular nitrogen coflow, as illustrated in Figure 3B. The flow rates of high-purity methane (99.95%) and ammonia (99.99%), oxygen (99.99%), and nitrogen (99.999%) were precisely controlled by the mass flow controllers (MFCs, Sevenstar D07) with $\pm 1\%$ accuracy. The MFCs were calibrated using a flow calibration instrument (Mesa

TABLE 1 Spectroscopic parameters of the original 24 lines of nitric oxide (NO) and the reduced two lines.

Original 24 lines			Reduced two line		
ν_0 (cm ⁻¹)	S_0 (393 k) (cm ⁻² ·atm ⁻¹)	E'' (cm ⁻¹)	ν_0 (cm ⁻¹)	$S_{0, \text{reduced}}$ (393 k) (cm ⁻² ·atm ⁻¹)	E_{reduced}'' (cm ⁻¹)
1900.0706	2.9790×10^{-1}	80.2188	1900.0740	1.8195	80.2596
1900.0706	3.4040×10^{-1}	80.2188			
1900.0706	2.5970×10^{-1}	80.2188			
1900.0720	5.3850×10^{-3}	80.2188			
1900.0721	5.3850×10^{-3}	80.2188			
1900.0736	2.4060×10^{-5}	80.2188			
1900.0772	2.4060×10^{-5}	80.3003			
1900.0792	5.3850×10^{-3}	80.3003			
1900.0796	5.3850×10^{-3}	80.3003			
1900.0816	3.4040×10^{-1}	80.3003			
1900.0816	2.5970×10^{-1}	80.3003			
1900.0816	2.9790×10^{-1}	80.3003			
1900.5164	1.4830×10^{-5}	202.2984	1900.5170	1.1212	202.2993
1900.5168	3.3227×10^{-3}	202.2984			
1900.5169	3.3227×10^{-3}	202.2984			
1900.5171	2.1030×10^{-1}	202.2984			
1900.5172	1.4830×10^{-5}	202.3001			
1900.5172	1.8346×10^{-1}	202.2984			
1900.5173	1.6017×10^{-1}	202.2984			
1900.5175	3.3227×10^{-3}	202.3001			
1900.5177	3.3295×10^{-3}	202.3001			
1900.5179	2.1030×10^{-1}	202.3001			
1900.5180	1.8346×10^{-1}	202.3001			
1900.5180	1.6017×10^{-1}	202.3001			

Laboratories, Defender510), with a measurement accuracy of 1%. By changing the flow rates of various gases, different flame conditions can be achieved. Note that, a stainless-steel plate was placed 21 mm above the burner to suppress flame flickering. The burner was mounted on a motorized linear translation stage (Yiheng, TDPF200) that moves vertically (4 mm interval) to facilitate spatially resolved measurements. During the measurements, a ceramic probe (KYOCERA_F121-11050-00700) with an inner diameter of 200 μm was fixed above the burner surface for gas sampling (shown in Figure 3C). The high-temperature gas cell was first pumped into the vacuum state and then the high-temperature flame gas was then filled into the gas cell due to the pressure difference between the gas cell and the target flame region. A pressure sensor (MIK P300) was used to monitor the absolute pressure in the gas cell. To prevent the condensation of water vapor during the sampling

process, the entire sampling pipeline and gas cells are heated and wrapped with insulating cotton to improve temperature uniformity. All heating equipment is regulated by PID control to maintain a temperature at 393 ± 1 K to ensure that the water vapor in the flue gases is in a gaseous state and will not condense during the sampling and measurement process.

4 | RESULTS AND DISCUSSION

Before presenting the measured NO results, we first present the performance of the proposed reduced model in fitting the measured absorption spectrum under different temperature and pressure conditions, as depicted in Figure 4A,B. Evidently, the fitting residuals obtained by employing the two equivalent absorption lines exhibit noticeably smoother

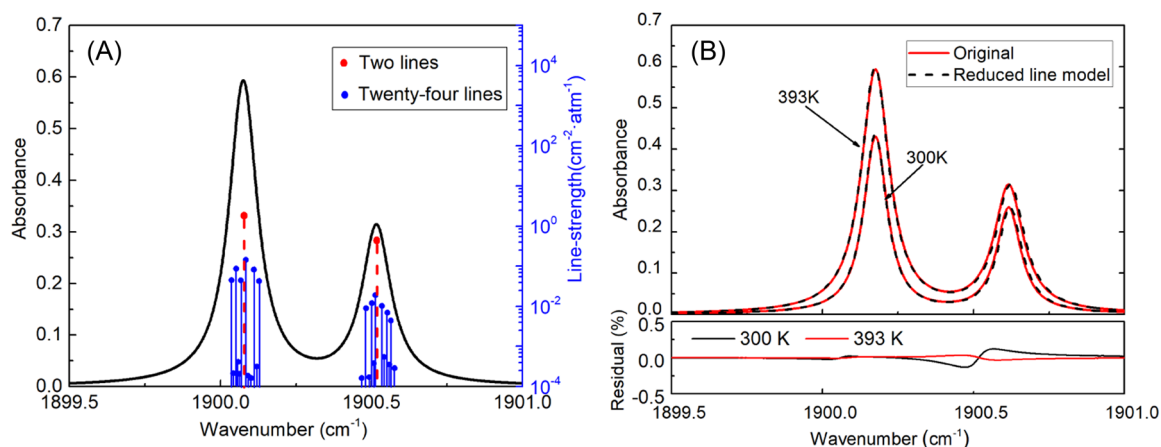


FIGURE 2 Demonstration of the reduced line model. (A) Absorption simulation of 1000 ppm nitric oxide (NO) at 393 K, 1 atm, and 35 cm path length using the six transitions. The line-strengths (at 393 K) are plotted as drop lines; (B) Comparison of simulated absorption spectra using the original 24 lines with that using the reduced two lines: 1000 ppm NH_3 , 1 atm, 35 cm path length, 300 K and 393 K. The relative difference is plotted at the bottom panel.

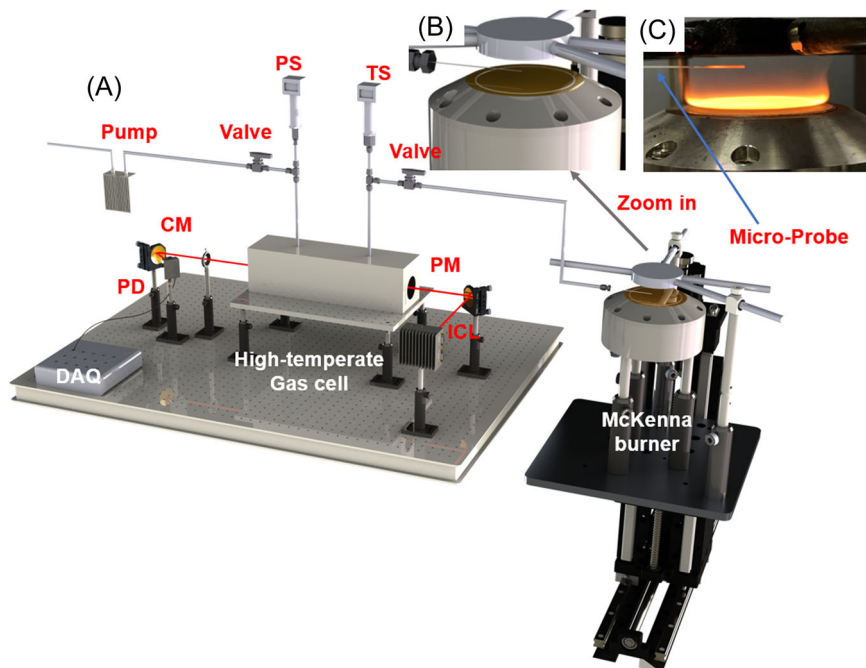


FIGURE 3 (A) Schematic of the optical configuration for nitric oxide (NO) measurements along with the representative image of laminar methane/ammonia/air flame. CM, concave mirror; DAQ, data acquisition module; ICL, interband cascade laser; PD, photodetector; PM, plane mirror; PS, pressure sensor; TS, temperature sensor; (B) Zoom in view of the burner; (C) Heated micro-probe within the flame.

curves and lower magnitudes compared to the residuals obtained from employing the 24 absorption lines. Furthermore, the convergence time for each measured spectrum using the two absorption lines is approximately 1.7 s, while the utilization of 24 absorption lines necessitates around 32 s, representing an approximately 19-fold increase in convergence time. The utilization of two equivalent absorption lines, as opposed to employing 24 absorption lines, offers a significant reduction in convergence time for Voigt-fitting, alongside an improved accuracy in the determination of the fitting-derived integrated absorbance.

First, standard gas mixtures of NO/N_2 with different NO concentrations were used to evaluate the measurement

performance of the developed sensor before applying the sensor for flame measurement. For standard gas mixtures, the NO concentration was precisely controlled from 200 to 4000 ppm using two thermal mass flow controllers and a standard gas cylinder (4000 ppm NO/N_2). Representative measurements of raw absorption spectra along with the Voigt fitting profiles for standard NO/N_2 mixtures were depicted in Figure 5A. All the target absorption features have a high signal-to-noise ratio and can be well-fitted by the Voigt function. The fractional Voigt-fitting residuals are less than 1.0% over the entire absorption feature. In particular, the residuals near the line-center of the selected absorption transitions were typically below 0.6%.

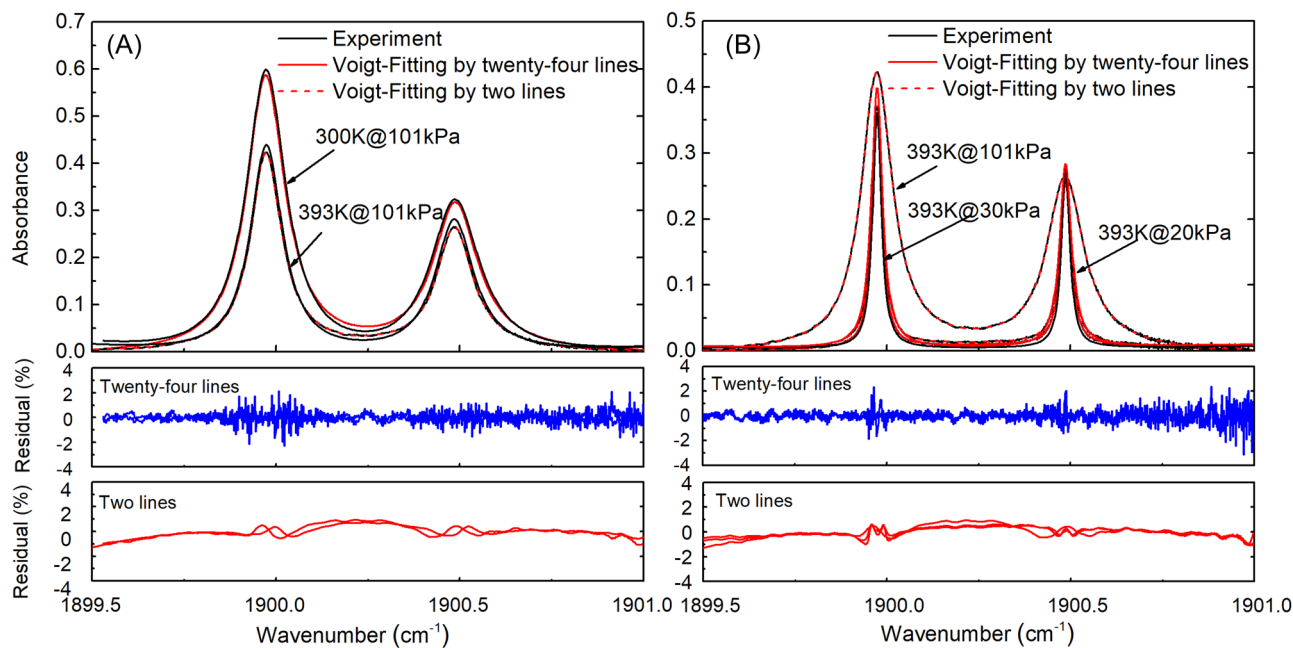


FIGURE 4 Comparisons of the Voigt-fitting performance using two equivalent absorption line and 24 absorption lines for (A) the pressure of 101 kPa with varied temperature (i.e., 300 K and 393 K); (B) the temperature of 393 K at varied pressure (i.e., 20, 30, and 101 kPa).

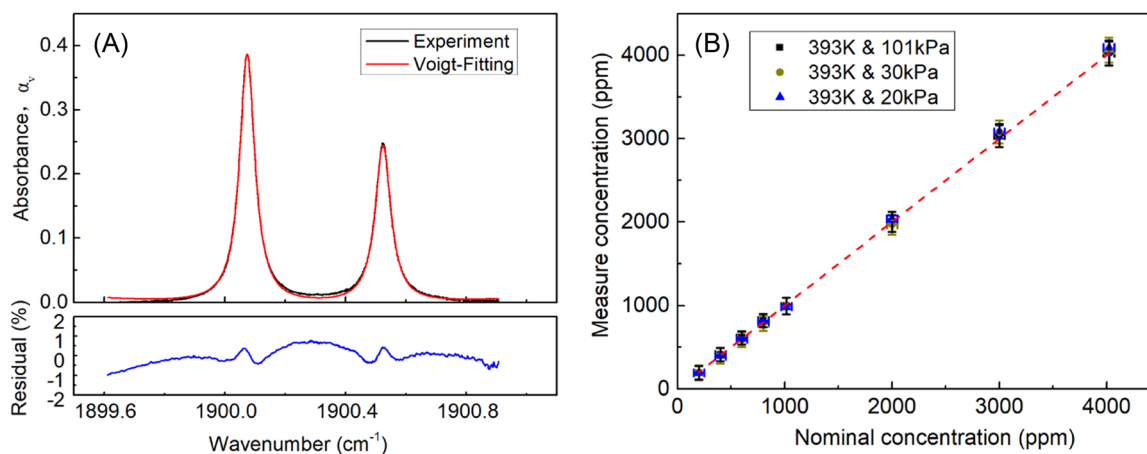


FIGURE 5 (A) Representative measured absorption profiles along with the best Voigt-fitting profiles for standard gas mixture of nitric oxide (NO) at 393 K, 30 kPa, and 1000 ppm. The residuals of the Voigt-fitting are presented at the bottom panels; (B) comparison of the measurement results to the nominal concentrations of NO at 20, 30, and 101 kPa.

Such small fitting residuals were also obtained for different concentrations in this study and indicate the reliable determination of integrated absorbance, which can ensure the precise and accurate results. Figure 5B compares the measurement results to the nominal concentrations range (200–4000 ppm) of NO at different pressures. Satisfactory agreements can be found between the measurement results and the nominal concentrations. The relative differences were mostly within 2.5% and the maximum value is ~4.0%, indicating that the developed sensor can provide accurate calibration-free measurement of high-temperature NO. Note

that the sampled gas flows into the gas cell with a relatively slow speed due to the rather small diameter of the sampling probe which can cause notable flow resistance. If NO was measured in a low-pressure way, the time for the high-temperature gas mixture from flame to fill in the gas cell can be significantly shortened. Therefore, for the flame measurements, the measured pressure was set at 30 kPa.

Allan deviation analysis was then performed to inspect the NO detection limit and stability of the sensor by continuously recording the measured peak absorption for 40 min. Pure nitrogen was fed to flow in the

high-temperature gas cell with a fixed temperature of 393 K. As shown in Figure 6, the developed sensor shows a minimum detection limit (MDL) of 2.02 ppm at the integration time of 1 s, which can be improved to

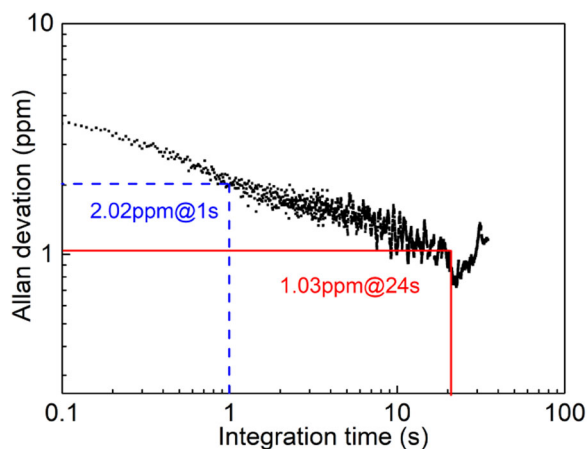


FIGURE 6 Allan deviation analysis of nitric oxide (NO) detection.

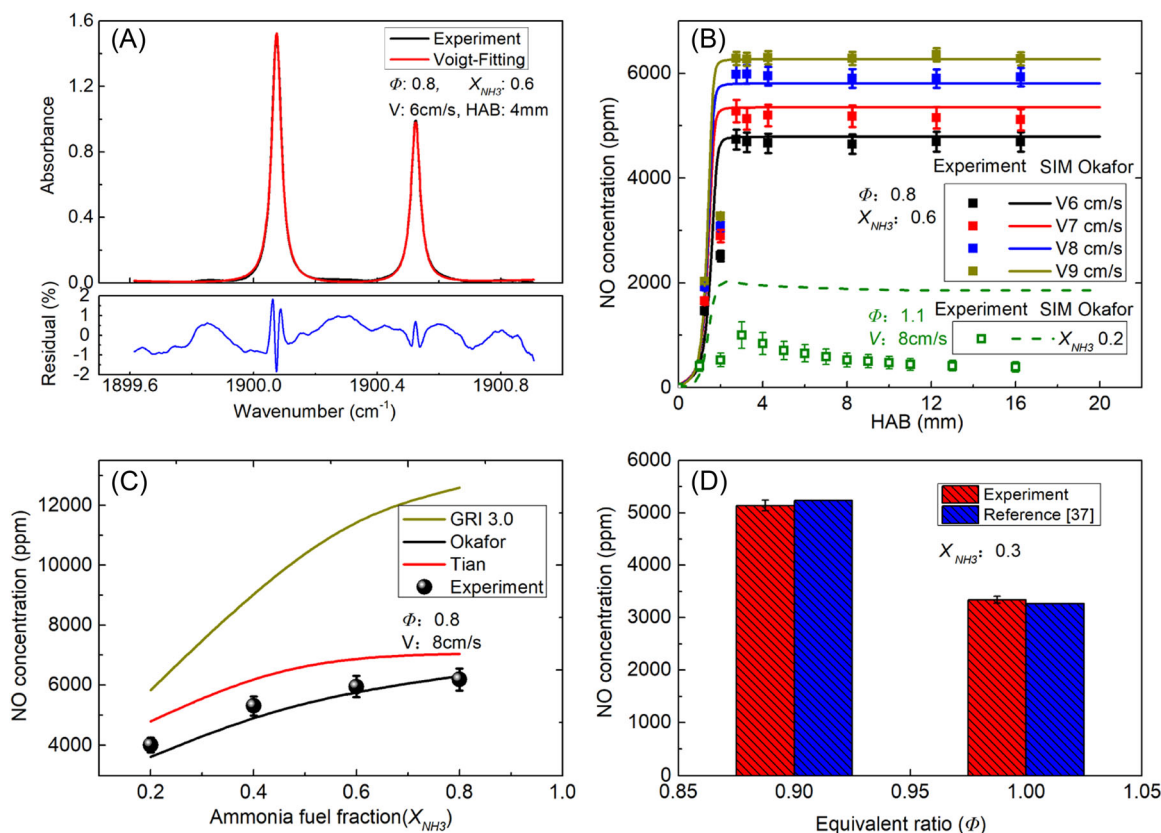


FIGURE 7 (A) Representative measured absorption profiles along with the best Voigt-fitting profiles for high-temperature gas mixtures sampled from flames; (B) measured and simulated nitric oxide (NO) concentration as a function of height above the burner (HAB) under flame condition of $\phi = 0.8$ and $X_{\text{NH}_3} = 0.6$ with different fuel mixture rate, and $\phi = 1.1$ and $X_{\text{NH}_3} = 0.2$; (C) measured and simulated NO concentration at HAB = 12 mm under flame condition of $\phi = 0.8$ with different NH_3 blending ratios; (D) comparisons of the measured NO concentration and the data from literature ($\phi = 0.9$, $X_{\text{NH}_3} = 0.3$, and $\phi = 1.0$, $X_{\text{NH}_3} = 0.3$).³⁷

1.03 ppm at the integration time of 24 s. Hence, the NO sensor is promising for NO measurement in ammonia-methane cofired flames where the NO concentration is at the concentration of a dozen ppm to thousands of ppm.

After demonstrating the measurement performance of the NO sensor against the standard gas mixtures, the sensor was used to measure the NO of laminar premixed methane-ammonia cofired flames. Additional kinetic modeling with different chemical mechanisms was performed for comparison against the experimental results. The modeling was conducted using the “Premixed Laminar Burner-Stabilized Stagnation Flame” module of the Chemkin package and the chemical mechanisms include GRI 3.0,³⁴ Tian and Cronstein³⁵ and Okafor mechanism.³⁶ Figure 7A shows the representative measurements of raw absorption spectra along with the Voigt fitting profiles for sampling mixtures from flames. Superior Voigt-fitting results with small fitting residuals indicates the high-fidelity for determination of NO concentration. Spatially measurements of NO in the flames with different flow rate of fuel mixture and equivalence ratio (ϕ) were illustrated in Figure 7B. Simulations using the Okafor mechanism were also presented. The increasing

tendency of NO when the fuel mixture increase was successfully captured by both our developed sensor and the kinetic modeling. For a fixed equivalence ratio of 0.8 and blending ratio of 0.6 at different flow rate of fuel mixtures (6–9 cm/s), the modeling results were in good agreement within measured results within 5%. When the equivalence ratio was switched from 0.8 to 1.1, the decreasing tendency of NO concentration along height above the burner (HAB) was experimentally captured. This is because selective noncatalytic reduction (SNCR) occurs downstream of the flame. The unburnt NH₃ reduced the generated NO. However, the kinetic modeling failed to predict such a phenomenon. Figure 7C shows the measured and simulated NO concentration at HAB of 12 mm in the post-flame region, where chemical reactions have already been completed and the NO concentration has reached the maximum value. It is clearly seen that NO increases as the NH₃ blending ratio (X_{NH_3}) increases, which is due to the more pronounced fuel-NO formation. The simulated results based on the Okafor mechanism were in good agreement with the measured value while the other two simulation results were much higher than the experimental measurements. Note that, experimental data by in situ broadband ultraviolet absorption measurements were also presented for comparisons,³⁷ as illustrated in Figure 7D. Our ex situ measurement results agree considerably well with in situ measurement results, indicating the additional minimally intrusive properties of our developed sensor.

5 | CONCLUSIONS

We have demonstrated the development of a mid-infrared absorption sensor for calibration-free and high-fidelity detection of nitric oxide (NO) at 5.2 μm in laminar premixed methane/ammonia cofired flames using a combination of a micro-probe and a low-pressure, high-temperature gas cell, which is particularly suitable for kinetic studies of ammonia combustion. An ICL was employed to detect the target the optimal NO absorption line near 1900.07 cm^{-1} . Calibration-free measurement of NO concentration was enabled using the DAS technique coupled with reduced a line model which improves the fitting efficiency in the presence of multifold transitions. By comprehensive measurements of the standard NO/N₂ mixture with known concentration at different pressures, the measurement accuracy was mostly within 2.5% and the measurement uncertainty was estimated to be 2.0%. The detection limit was achieved to be ~ 2 ppm at the integration time of 1 s. The application of the sensor for NO measurement in methane-ammonia flames was then carried out and our developed sensor successfully captured the increasing tendency of NO concentration when the NH₃ blending ratio and flow rate of fuel mixture increases. In

addition, the measured data can act as the benchmark for the evaluation of chemical mechanisms. The good agreements with the in situ measurement results from literature also demonstrated the minimally intrusive property of the developed sensor. To conclude, the developed sensor can be applied for quantitative and spatially resolved measurement of NO concentration in an ammonia-methane cofired flame with superior accuracy, sensitivity and fidelity, which provides a new alternative measurement tool for kinetics study of NO formation.

ACKNOWLEDGMENTS

This research is supported by the National Natural Science Foundation of China (NSFC) (52106221, 51976142), the State Key Laboratory of Applied Optics (SKLA02022001A05) and Foshan Xianhu Laboratory of the Advanced Energy Science and Technology Guangdong Laboratory (XHD2022-001).

DATA AVAILABILITY STATEMENT

The data that support the findings of this study are available from the corresponding author upon reasonable request.

ORCID

Yu Wang  <http://orcid.org/0000-0001-8795-9174>

REFERENCES

1. Kobayashi H, Hayakawa A, Somarathne KDKA, Okafor EC. Science and technology of ammonia combustion. *Proc Combust Inst.* 2019;37(1):109-133.
2. Chai WS, Bao Y, Jin P, Tang G, Zhou L. A review on ammonia, ammonia-hydrogen and ammonia-methane fuels. *Renew Sustain Energy Rev.* 2021;147:111254.
3. Elbaz AM, Wang S, Guiberti TF, Roberts WL. Review on the recent advances on ammonia combustion from the fundamentals to the applications. *Fuel Commun.* 2022; 10:100053.
4. Okafor EC, Somarathne KDKA, Ratthan R, et al. Control of NO_x and other emissions in micro gas turbine combustors fuelled with mixtures of methane and ammonia. *Combust Flame.* 2020;211:406-416.
5. Brown MD, Schoenfish MH. Electrochemical nitric oxide sensors: principles of design and characterization. *Chem Rev.* 2019;119(22):11551-11575.
6. Dinh TV, Choi IY, Son YS, Kim JC. A review on non-dispersive infrared gas sensors: improvement of sensor detection limit and interference correction. *Sens Actuators, B.* 2016;231:529-538.
7. Peng R, Liu WQ, Fang W, Sun YW. [Measurement and analysis of nitric oxide gas based on the algorithm of non-dispersive ultra-violet]. *Guang pu xue yu guang pu fen xi = Guang pu.* 2012;32(12):3381-3384.
8. Bak J, Clausen S. FTIR emission spectroscopy methods and procedures for real time quantitative gas analysis in industrial environments. *Meas Sci Technol.* 2001;13(2): 150-156.

9. Taha Z. Nitric oxide measurements in biological samples. *Talanta*. 2003;61(1):3-10.
10. Thomas DE, Shrestha KP, Mauss F, Northrop W. Extinction and NO formation of ammonia-hydrogen and air non-premixed counterflow flames. *Proceedings of the Combustion Institute*. 2022.
11. Hayakawa A, Hirano Y, Okafor EC, Yamashita H, Kudo T, Kobayashi H. Experimental and numerical study of product gas characteristics of ammonia/air premixed laminar flames stabilized in a stagnation flow. *Proc Combust Inst*. 2021;38(2):2409-2417.
12. Bradley KS, Brooks KB, Hubbard LK, Popp PJ, Stedman DH. Motor vehicle fleet emissions by OP-FTIR. *Environ Sci Technol*. 2000;34(5):897-899.
13. Leippe G, Lenzen B, Spurk P, et al. A new system for measuring the nitrogen components N₂O, NH₃, NO and NO₂ downstream of DeNOX catalytic converters. *MTZ Worldw*. 2004;65(5):23-27.
14. Schulz C, Sick V. Tracer-LIF diagnostics: quantitative measurement of fuel concentration, temperature and fuel/air ratio in practical combustion systems. *Prog Energy Combust Sci*. 2005;31(1):75-121.
15. He Q, Chang J, Li M, Li J, Feng Q. Oxygen detection based on Faraday modulation spectroscopy and wavelength modulation spectroscopy: a comparison. *Microw Opt Technol Lett*. 2023;65(5):1353-1358.
16. Farooq A, Alqaity ABS, Raza M, Nasir EF, Yao S, Ren W. Laser sensors for energy systems and process industries: perspectives and directions. *Prog Energy Combust Sci*. 2022;91:100997.
17. Cai W, Kaminski CF. Tomographic absorption spectroscopy for the study of gas dynamics and reactive flows. *Prog Energy Combust Sci*. 2017;59:1-31.
18. Ma Y, Liang T, Qiao S, Liu X, Lang Z. Highly sensitive and fast hydrogen detection based on light-induced thermoelastic spectroscopy. *Ultrafast Sci*. 2023;3:0024.
19. Liu X, Ma Y. Tunable diode laser absorption spectroscopy based temperature measurement with a single diode laser near 1.4 μm . *Sensors*. 2022;22(16):6095.
20. Sheng G, Han J, Ma L, Wang W, Wang Y. Mid-infrared multiline absorption tomography for in situ analysis of thermochemical structure in natural gas-fired cooker flame. *Microw Opt Technol Lett*. 2023;65(5):1215-1222.
21. Li J, Wang Z, Yu Z, Li L, Yang X, He L. Wavelength modulation-based active laser heterodyne spectroscopy for standoff gas detection. *Microw Opt Technol Lett*. 2023;65(5):1261-1270.
22. Chen W, Qiao S, Zhao Z, Gao S, Wang Y, Ma Y. Sensitive carbon monoxide detection based on laser absorption spectroscopy with hollow-core antiresonant fiber. *Microw Opt Technol Lett*, 2023. doi:10.1002/mop.33780
23. Ma LH, Lau LY, Ren W. Non-uniform temperature and species concentration measurements in a laminar flame using multi-band infrared absorption spectroscopy. *Appl Phys B*. 2017;123:83.
24. Chuan T, Lichang Z, Bin R, et al. Optimization method research on low NO concentration detection by mid-infrared TDLAS based on EMD. *Chin J Quant Electron*. 2021;38(5):661.
25. Wen D, Wang Y. Spatially and temporally resolved temperature measurements in counterflow flames using a single interband cascade laser. *Opt Exp*. 2020;28(25):37879-37902.
26. Nie W, Xu Z, Rao G, et al. Methods of tunable diode laser absorption saturation spectroscopy to gas sensing under optically thick conditions. *Microw Opt Technol Lett*. 2021;63(8):2063-2067.
27. Chao X, Jeffries JB, Hanson RK. Wavelength-modulation-spectroscopy for real-time, in situ NO detection in combustion gases with a 5.2 μm quantum-cascade laser. *Appl Phys B*. 2012;106:987-997.
28. Almodovar CA, Spearrin RM, Hanson RK. Two-color laser absorption near 5 μm for temperature and nitric oxide sensing in high-temperature gases. *J Quant Spectrosc Radiat Transfer*. 2017;203:572-581.
29. Diemel O, Pareja J, Dreizler A, Wagner S. An interband cascade laser-based in situ absorption sensor for nitric oxide in combustion exhaust gases. *Appl Phys B*. 2017;123:167.
30. Duan K, Ji Y, Wen D, Lu Z, Xu K, Ren W. Mid-infrared fiber-coupled laser absorption sensor for simultaneous NH₃ and NO monitoring in flue gases. *Sens Actuators B*. 2023;374:132805.
31. Hanson R, Spearrin R, Goldenstein C. *Spectroscopy and optical diagnostics for gases*. Springer; 2016;1.
32. McLean AB, Mitchell CEJ, Swanston DM. Implementation of an efficient analytical approximation to the Voigt function for photoemission lineshape analysis. *J Electron Spectrosc Relat Phenom*. 1994;69(2):125-132.
33. Gordon IE, Rothman LS, Hargreaves RJ, et al. The HITRAN2020 molecular spectroscopic database. *J Quant Spectrosc Radiat Transfer*. 2022;277:107949.
34. Smith GP, Golden DM, Frenklach M, et al. GRI 3.0 Mechanism. <http://combustion.berkeley.edu/gri-mech/>
35. Tian H, Cronstein BN. Understanding the mechanisms of action of methotrexate. *Bull NYU Hosp Jt Dis*. 2007;65(3):168-173.
36. Okafor EC, Naito Y, Colson S, et al. Experimental and numerical study of the laminar burning velocity of CH₄-NH₃-air premixed flames. *Combust Flame*. 2018;187:185-198.
37. Yang X, Peng Z, Ding Y, Du Y. Spatially resolved broadband absorption spectroscopy measurements of temperature and multiple species (NH, OH, NO, and NH₃) in atmospheric-pressure premixed ammonia/methane/air flames. *Fuel*. 2023;332:126073.

How to cite this article: Li Q, Ji F, Wang W, Ma L, Wang Y. A mid-infrared laser absorption sensor for calibration-free measurement of nitric oxide in laminar premixed methane/ammonia cofired flames. *Microw Opt Technol Lett*. 2024;66:e33815. doi:10.1002/mop.33815